Equilibrium, stability and evolution of bubbles in a finite melt volume

D. R. Jenkins[1] J. Kiely[2]

(Received 9 January 2012; revised 16 June 2012)

Abstract

We consider a simple model of the simultaneous expansion and/or contraction of multiple bubbles, initially having the same size, immersed in a finite melt volume. The bubble growth is due to the presence of a dissolved gas within the melt. The model has multiple equilibria, and we examine the stability of each equilibrium state, via linear stability analysis and numerical experiment. We show that in every case it is the largest bubble size that is stable. Finally, we consider a generalisation of the model which allows a demonstration of the process of Ostwald ripening, where smaller bubbles contract while larger bubbles expand. The model has application to a diverse range of phenomena, including the head on a glass of beer, magma systems and the conversion of coal into coke.

http://journal.austms.org.au/ojs/index.php/ANZIAMJ/article/view/5102 gives this article, © Austral. Mathematical Soc. 2012. Published August 8, 2012. ISSN 1446-8735. (Print two pages per sheet of paper.)

Contents

1 Introduction

There are several instances in natural and man-made materials where the existence of a large number of bubbles has significant effect on the behaviour or performance of a system. Examples include magma systems, where the formation and expansion of bubbles is directly responsible for explosive ejection of material from the system [1]; the 'head' on a glass of beer, which consists of a 'wet' foam containing large numbers of bubbles [2]; the formation of coke from coal, where volatile gases in the softened coal promote the growth of bubbles, which in turn have a significant effect upon the structural properties of the coke [3]. In each of these cases, it is necessary to consider the behaviour of a large number of bubbles, rather than a single, isolated bubble, in order to understand the behaviour of the system. Some studies of multiple bubble systems consider distributions of bubble sizes and their evolution through time via population equations [4], whereas others consider all of the bubbles to be the same, but arranged in a way that their interaction is taken into account [5, 6]. We take the latter approach, in order to investigate the existence of equilibrium states for a representative multiple bubble system,

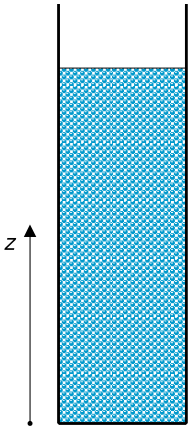

Figure 1: Schematic of a fluid-bubble mixture in a cylinder.

and then examine the stability of the equilibria. The aim is to use such a model to identify key features of the different systems, by means of a particularly simple model. Finally, we generalise the simple model to demonstrate a feature of this type of system called Ostwald ripening [7].

2 Monomodal model

Consider a set of N bubbles, each locally having the same radius $R(z)$ and internal gas pressure p_g, distributed uniformly throughout a fixed volume V_m of viscous fluid. We find it convenient to consider the fluid-bubble mixture to be contained within a circular cylinder of diameter d, closed at the bottom but free to move at the top, as shown in Figure 1. The total volume of the sample is

$$V = \frac{\pi d^2}{4} h = V_m + \frac{4}{3} N \pi R^3, \tag{1}$$

from which the height of the sample is obtained. Such a cylinder could be a vertical conduit through rock for volcanic magma, the dilatometer column used for assessing the properties of coking coal [3], or the head on a glass of carbonated drink, such as beer. For simplicity, we consider the bubbles to be locally positioned in a face centred cubic (FCC) arrangement, where the side of the standard cube is of length S. Then, taking the approach of, for example, Proussevich et al. [5], we obtain a set of equations for the growth of the bubbles:

$$\frac{dR}{dt} = \frac{(p_g - p_f - 2\gamma/R)RS^3}{4\mu(S^3 - 8R^3)}, \tag{2}$$

$$\frac{d}{dt}(R^3 p_g) = \frac{6R_g T R^2 D\rho}{SM}(C - C_s), \tag{3}$$

$$(1-\epsilon)\frac{DC}{Dt} = D\frac{\partial^2 C}{\partial z^2} - \frac{8\pi n D R^2}{S}(C - C_s), \tag{4}$$

where μ is the melt viscosity, t is elapsed time, p_f is the pressure of the fluid, R_g is the universal gas constant, T is the absolute temperature, D is the diffusion coefficient of the gas within the fluid, ρ is the fluid density, C is the mass fraction of gas in the fluid bulk, C_s is the equilibrium concentration of gas on the surface of the bubbles, M is the molecular weight of the gas, and n is the number density of the bubbles. The first equation is a momentum balance where inertial terms are neglected. The following two equations consider that the growth or collapse of the bubbles is due to the presence of absorbed (ideal) gas within the surrounding melt, being equations for the conservation of gas within the bubbles and the melt, respectively. Gas transport in the melt is via diffusion through the bulk of the melt, which is the first term on the right of Equation (3), or transport into bubbles, given by the second term. The second term is obtained by assuming that flux of gas into the bubbles is $(C - C_s)D/(2S)$, which depends on the half-spacing between bubbles. This is a simplification of the actual diffusion of gas, but it is practically reasonable. Note that, given the cylindrical volume, we consider that the bubble radius, gas pressure and gas concentration in the melt are all functions of the vertical position z and time t only. Moreover, we consider

that gas escapes through the top surface of the sample, so that the flux of gas at $z = h$ is

$$D \left.\frac{\partial C}{\partial z}\right|_{z=h} = h_s C_s(h). \tag{5}$$

The equilibrium gas concentration on the bubble surface is determined by Henry's Law, which relates it to the bubble gas pressure,

$$C_s = (K_h p_g)^\eta, \tag{6}$$

and we specifically consider the two cases $\eta = 1$ and $\eta = 0.5$. According to Proussevitch et al. [5], $\eta = 0.5$ is appropriate for water dissolved in a basaltic melt, whereas $\eta = 1$ is appropriate for CO_2 dissolved in water [8]. We define the volume fraction of bubbles as

$$\epsilon = \frac{\frac{4}{3}N\pi R^3}{V_m + \frac{4}{3}N\pi R^3}. \tag{7}$$

3 Equilibrium solutions

In the case where there is no gas loss from the surface of the melt, that is, $h_s = 0$, there are equilibrium solutions where all bubbles are of the same radius, R. In this case, the equilibrium is

$$p_g = p_f + \frac{2\gamma}{R}, \tag{8}$$

$$C = C_s = (K_h p_g)^\eta. \tag{9}$$

If the bubbles initially each have radius R_0 and gas pressure p_{g0}, then conservation of gas in the system requires that any equilibrium solution needs to satisfy

$$\rho\, C V_m + N\frac{4}{3}\pi R^3 \frac{p_g M}{R_g T} = \rho\, C_0 V_m + N\frac{4}{3}\pi R_0^3 \frac{p_{g0} M}{R_g T}. \tag{10}$$

Combining (8), (9) and (10) gives the following fourth order polynomial for r ($\eta = 1$)

$$\left(\alpha\omega\frac{1-\epsilon_0}{\epsilon_0} + r^3\right)(\delta r + 1) = \left(\alpha\omega\frac{1-\epsilon_0}{\epsilon_0} + 1\right)(\delta + 1)r \tag{11}$$

where

$$r = \frac{R}{R_0}, \quad \alpha = \frac{\rho R_g T}{p_f M}, \quad \delta = \frac{p_f R_0}{2\gamma}, \quad \omega = p_f K_h,$$

or gives the seventh order polynomial for r ($\eta = 0.5$)

$$\left[\alpha\frac{1-\epsilon_0}{\epsilon_0}\right]^2 \omega\delta(\delta r + 1) = r\left[\alpha\frac{1-\epsilon_0}{\epsilon_0}\sqrt{\omega\delta(\delta+1)} + (\delta+1) - r^2(\delta r + 1)\right]^2. \tag{12}$$

Both Equations (11) and (12) have the trivial solution $r = 1$, as well as one other positive real solution. In the case of $\eta = 1$ the other positive real solution is only feasible if

$$\delta > \frac{\alpha\frac{1-\epsilon_0}{\epsilon_0} - r_1^2 - r_1}{r_1^3 + r_1^2 + r_1}, \tag{13}$$

where

$$r_1 = \frac{1-\epsilon_0}{\epsilon_0}\frac{\pi}{3\sqrt{2}-\pi}$$

corresponds to the dimensionless bubble radius when all the bubbles are touching in the FCC configuration, at which point $\epsilon = \frac{\pi}{3\sqrt{2}}$.

A similar, though more complicated, constraint applies to the second solution in the $\eta = 0.5$ case. Note that the second solution, having $r \neq 1$, can be achieved because the total volume, V, of the system changes according to Equation (1).

For illustrative purposes, we consider the examples of dissolved CO_2 in water at 298 K ($\eta = 1$) and dissolved H_2O in basaltic melt ($\eta = 0.5$). Table 1 shows the appropriate parameters for these two cases.

Table 1: Properties of the two example systems considered.

	CO_2 in water $\eta = 1$	basaltic melt $\eta = 0.5$
K_h (Pa^{-1})	1.48×10^{-8}	5×10^{-11}
ρ (kg/m^3)	1000	2600
γ (N/m)	0.3	0.36
T (K)	298	1273

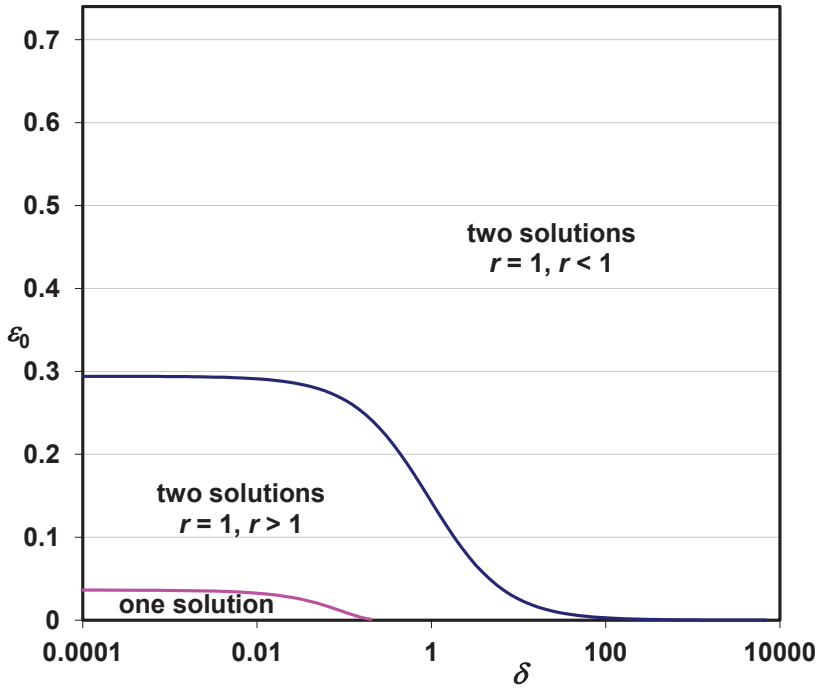

Figure 2: One of four graphs showing the regions of (δ, ϵ_0) space in which one or two equilibria exist for the data of Table 1 and the case $\eta = 1$.

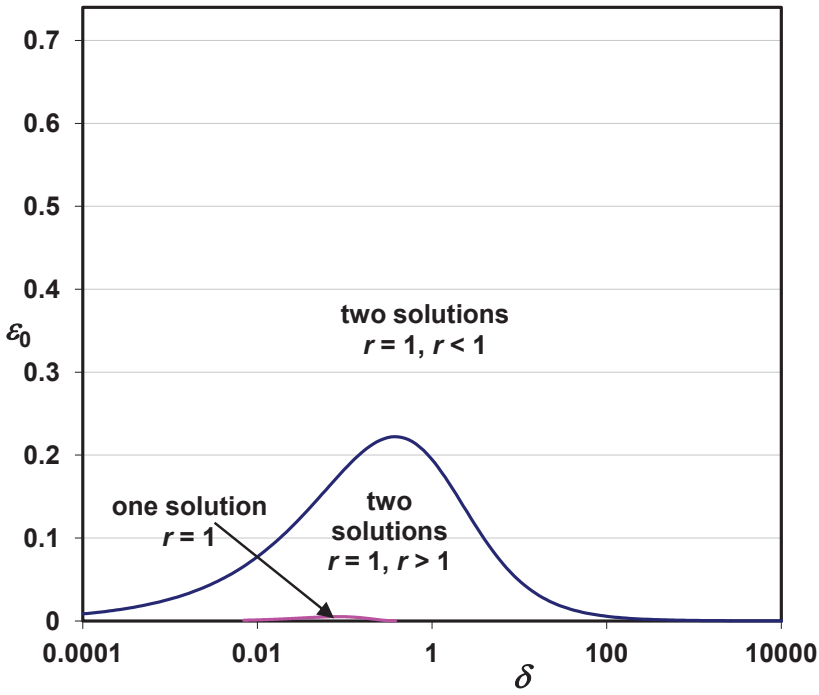

Figure 3: One of four graphs showing the regions of (δ, ϵ_0) space in which one or two equilibria exist for the data of Table 1 and the case $\eta = 0.5$, $p_f = 10\,\text{MPa}$.

Figurs 2–5 shows the different regions of (δ, ϵ_0) space in which feasible solutions exist for the two cases in Table 1. Also shown in each graph is the boundary between regions where the second solution has $r < 1$, at higher voidages, and $r > 1$ at lower voidages. This is the locus along which $r = 1$ is a double root of the equilibrium equation(s)

$$3\delta + 2 = \alpha\omega \frac{1 - \epsilon_0}{\epsilon_0}, \tag{14}$$

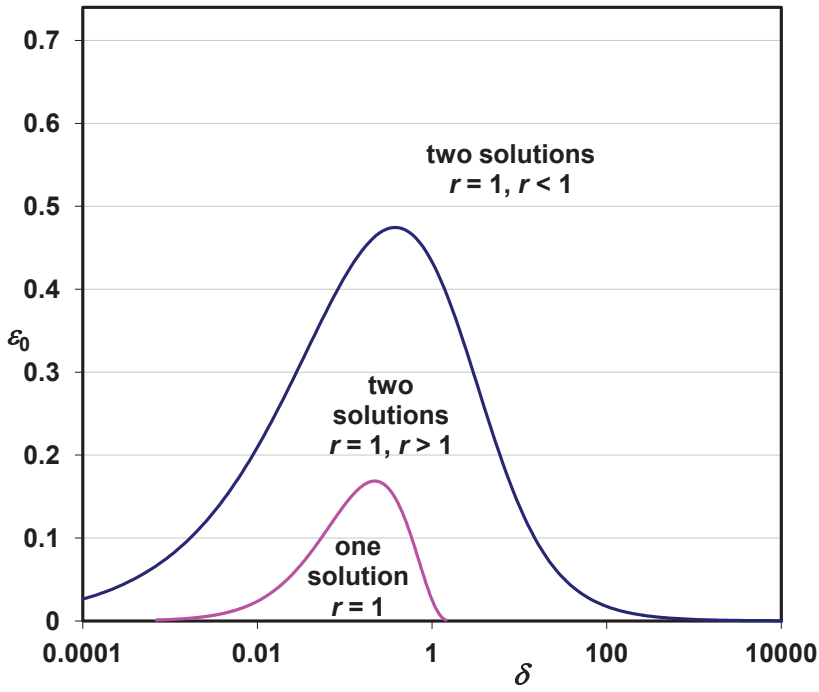

Figure 4: One of four graphs showing the regions of (δ, ϵ_0) space in which one or two equilibria exist for the data of Table 1 and the case $\eta = 0.5$, $p_f = 1$ MPa.

for $\eta = 1$ and

$$3\delta + 2 = \alpha \frac{1 - \epsilon_0}{\epsilon_0} \frac{\sqrt{\omega\delta}}{2\sqrt{\delta + 1}}, \tag{15}$$

for $\eta = 0.5$.

The graphs show that the different forms of Henry's Law lead to quite different possibilities for equilibrium. In the $\eta = 1$ case (Figure 2), two solutions exist for a wide range of situations, while a single solution ($r = 1$) exists for small bubble sizes at low voidage. In the $\eta = 0.5$ case, results are shown for three

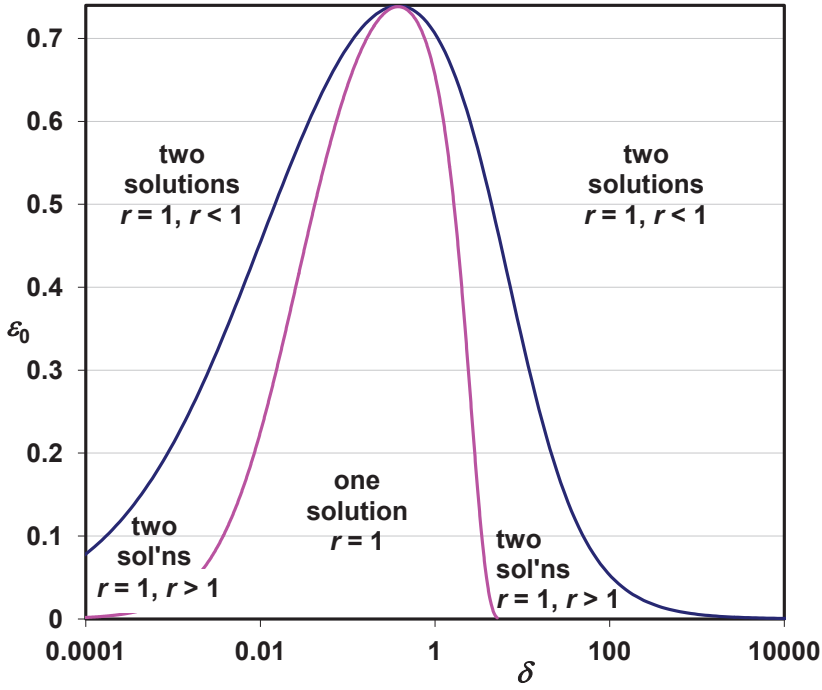

Figure 5: One of four graphs showing the regions of (δ, ϵ_0) space in which one or two equilibria exist for the data of Table 1 and the case $\eta = 0.5$, $p_f = 0.1013$ MPa.

different pressures, effectively representing the situation for different depths of basaltic melt. Figure 3 represents the situation a few hundred metres down into a melt. The region below the pink curve, where bubbles are unstable and grow to bursting, is extremely small, indicating that bubbles at depth are very stable. At a few tens of metres down (Figure 4), there is a moderate sized region of the space where the bubbles are unstable, but at the surface (Figure 5), the unstable region is very large, indicating the explosive potential of bubbles near the surface.

All of these solutions make the assumption that there is sufficient gas dissolved in the melt for the equilibria to actually exist. For small bubbles, this becomes unlikely because the required gas concentration increases as bubble size decreases, as a consequence of Equations (8) and (9).

4 Stability and Ostwald ripening

Linear stability of each the equilibria was considered by using Equations (2) and (3) along with (10), which holds at all times. Evaluation of the Jacobian of the right hand side of the resulting pair of ODEs at the equilibrium points shows that, in the region where only the $r = 1$ solution exists, it is always unstable to small perturbations. This is likely to mean that bubbles in this state grow until they touch and then will likely coalesce to form fewer, larger bubbles. In the regions where two equilibria are possible, we find that the solution with the smaller radius is always unstable, while the one with the larger radius is always stable. This situation holds for both $\eta = 1$ and $\eta = 0.5$. Accordingly, the boundaries shown in Figures 2–5 also represent stability boundaries. Similar results on existence and stability of bubble equilibria were found by Ward et al. [8]. The stability we are considering here, given the system of equations used, is equivalent to all of the bubbles in the system being perturbed in the same way. In order to further investigate stability, we consider the case where two equilibria exist, and examine what happens when the smaller bubbles are perturbed, by numerical solution of (2) and (3). Figure 6 shows the result in one particular example. In this case, the initial equilibrium was perturbed by slightly changing the bubble radius from its equilibrium, then adjusting the initial gas pressure so that the total gas in the system is conserved. As a result, we see that the bubbles grow in size until they reach a different equilibrium which is stable numerically. This equilibrium is the other solution of Equation (12).

In order to relax the stability condition somewhat, we consider the equilibrium FCC configuration of bubbles to consist of two populations, one being the

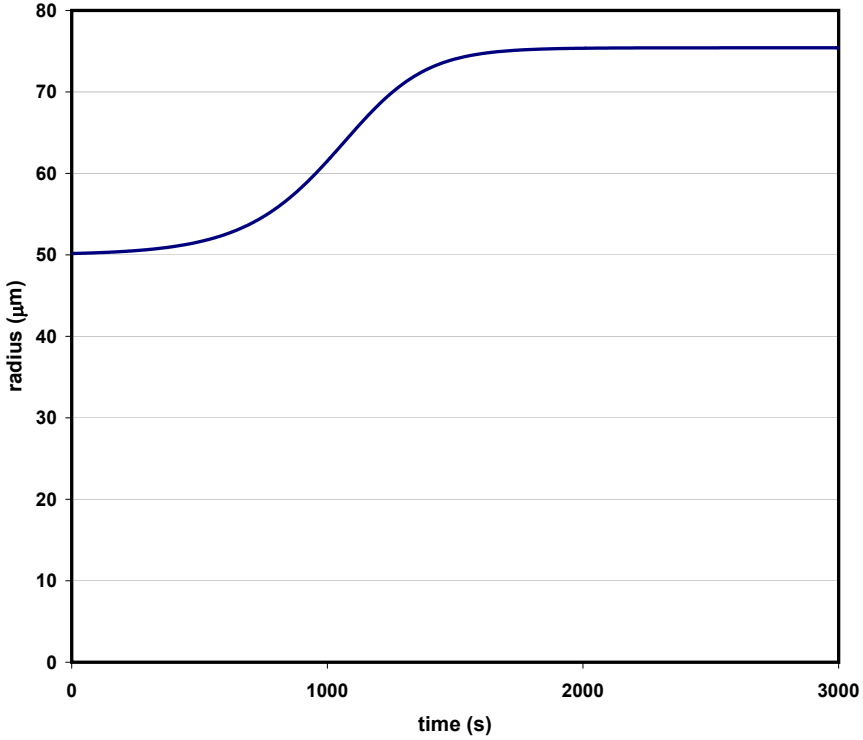

Figure 6: Time evolution from an unstable state with bubbles of initial radius, $R_0 = 50\,\mu m$ and $\epsilon_0 = 0.25$. The simulation is for the case $\eta = 0.5$, $p_f = 0.1013\,MPa$.

bubbles on the vertices of the unit cube, having radius R_1 and internal gas pressure p_{g1}, and the other being the bubbles on the faces of the unit cube, having radius R_2 and internal gas pressure p_{g2}. Then we generalise Equations (2) and (3) to

$$\frac{dR_1}{dt} = \frac{(p_{g1} - p_f - 2\gamma/R_1)R_1S^3}{4\mu(S^3 - (R_1 + R_2)^3)}, \tag{16}$$

$$\frac{dR_2}{dt} = \frac{(p_{g2} - p_f - 2\gamma/R_2)R_2S^3}{4\mu(S^3 - (R_1 + R_2)^3)}, \tag{17}$$

$$\frac{d}{dt}(R_1^3 p_{g1}) = \frac{6R_gTR_1^2D\rho}{SM}(C - C_{s1}), \tag{18}$$

$$\frac{d}{dt}(R_2^3 p_{g2}) = \frac{6R_gTR_2^2D\rho}{SM}(C - C_{s2}). \tag{19}$$

These equations have the same equilibria and linear stability behaviour as the previous ones. Note that for equilibrium, they need to have $R_1 = R_2$. Finally, we solve these equations numerically, with an initial condition being an unstable equilibrium point, in the region where two equilibria exist, but having the radius of one set of bubbles R_1 perturbed slightly from equilibrium, again perturbing p_{g1} in order to conserve the total mass of gas. The result is shown in Figure 7, which shows that one set of bubbles shrink and eventually collapse, while the other set of bubbles grow, eventually reaching a new equilibrium solution. This, then, is a clear demonstration of the condition known as Ostwald ripening, where larger bubbles tend to grow at the expense of their smaller neighbours, which collapse. The reason in this case is that, whenever there is a difference in bubble sizes, a concentration gradient is set up between the bubbles, and gas will diffuse in the direction of the larger bubble, because it has a lower gas concentration on its surface.

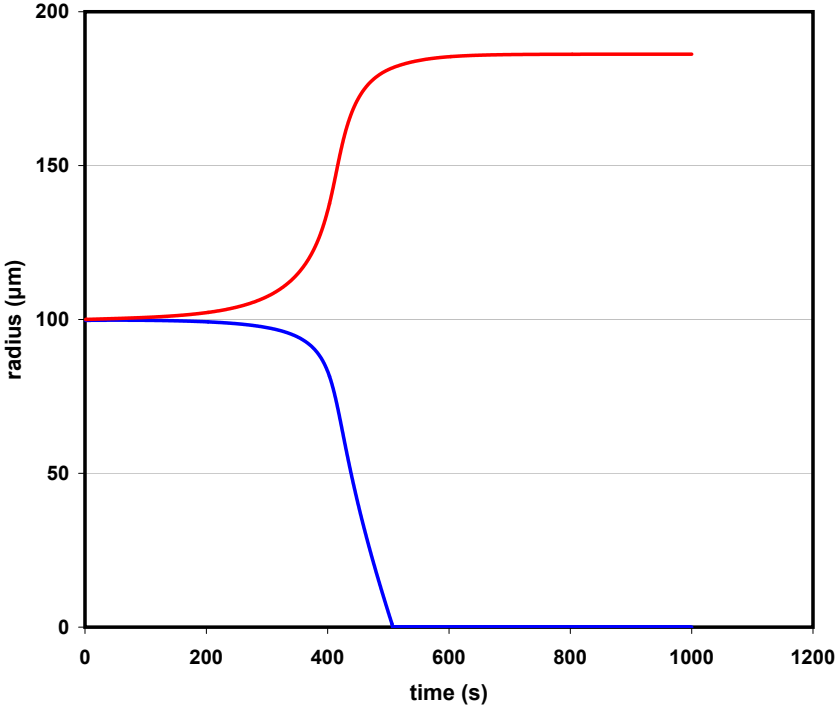

Figure 7: Time evolution of a bimodal bubble distribution, showing a model of Ostwald ripening.

5 Conclusions

The model for equilibrium and stability presented here could be argued to be overly simplistic, especially given we assume all bubbles have the same size and are arranged in a regular fashion. However, it has been shown in population dynamics models of multiple bubbles that solutions tend towards monomodal systems in the case when the fluid viscosity is low or extremely high [4] and also that collections of monodisperse bubbles self-organise into regular crystalline (FCC) arrangements [9, 10]. We emphasise that stability

will be compromised in real systems by factors not considered here, especially gravity (which leads to drainage of liquid from the foam). Moreover, we have not considered processes that lead to the formation of bubbles (nucleation) or their destruction (for example, by coalescence).

References

[1] H. M. Gonnermann & M. Manga, The fluid mechanics inside a volcano. *Annu. Rev. Fluid Mech.* **39** (2007) 321–356. doi:10.1146/annurev.fluid.39.050905.110207 C479

[2] K. Malysa, Wet foams: formation, properties and mechnism of stability. *Adv. Colloid Interface Sci.* **40** (1992) 37–83. doi:10.1016/0001-8686(92)80071-5 C479

[3] R. Loison, P. Foch, A. Boyer, *Coke: Quality and Production.* 2nd Ed. 1989. Butterworths. C479, C481

[4] K. Yamada, H Emori, K Nakazawa, Time-evolution of bubble formation in a viscous liquid. *Earth Planets Space* (2008) **60**, 661–679. C479, C491

[5] A. A. Proussevitch, D. L. Sahagian, A. T. Anderson, Dynamics of diffusive bubble growth in magmas: Isothermal case. *J. Geophys. Res.* (1993) **98**(B12), 22283–22307. doi:10.1029/93JB02027 C479, C481, C482

[6] A. A. Proussevitch, D. L. Sahagian, Dynamics and energetics of bubble growth in magmas: analytical formulation and numerical modeling. *J. Geophys. Res.* (1998) **103**(B8), 18223–18251. doi:10.1029/98JB00906 C479

[7] P. Stevenson, Inter-bubble gas diffusion in liquid foam. *Current Opinion in Colloids and Interface Sci.* (2010) **15**, 374–381. doi:10.1016/j.cocis.2010.05.010 C480

[8] C. A. Ward, P. Tikuisis, R. D. Venter. Stability of bubbles in a closed volume of liquid-gas solution. *J. Appl. Phys.* (1982) **53**(9), 6076–6084. doi:10.1063/1.331559 C482, C488

[9] A. van der Net, W. Drenckhan, D. Weaire, S. Hutzler, The crystal structure of bubbles in the wet foam limit. *Soft Matter* (2006) **2**, 129–134. doi:10.1039/b515537a C491

[10] A. van der Net, G. W. Delaney, W. Drenckhan, D. Weaire, S. Hutzler, Crystalline arrangements of microbubbles in monodisperse foams. *Coll. Surf. A: Physicochem. Eng. Aspects* (2007) **309**, 117–124. doi:10.1016/j.colsurfa.2006.11.056 C491

Author addresses

1. **D. R. Jenkins**, CSIRO Mathematics, Informatics and Statistics, Locked Bag 17, North Ryde NSW 1670, Australia.
mailto:David.Jenkins@csiro.au

2. **J. Kiely**, CSIRO Mathematics, Informatics and Statistics, Locked Bag 17, North Ryde NSW 1670, Australia.